Laminar Forced Convection of Dusty Air through Porous Media in a Vertical Annulus

Asst. Prof. Dr. Manal Hadi salh AL-Hafidh
Engineering College-Baghdad University
Email: manal hadi2005@yahoo.com

Salman Hameed Obaid
Engineering College-Baghdad University
E-mail: moment_1989@yahoo.com

ABSTRACT

An experimental and numerical study has been carried out to investigate the forced convection heat transfer by clean or dusty air in a two dimensional annulus enclosure filled with porous media (glass beads) between two vertical concentric cylinders. The outer cylinder is of (82 mm) outside diameters and the inner cylinder of (27 mm) outside diameter. Under steady state condition; the inner cylinder surface is maintained at a high temperature by applying a uniform heat flux and the outer cylinder surface at an ambient temperature. The investigation covered values of input power of (6.3, 4.884, 4.04 and 3.26 W), Reynolds number values of (300, 700, 1000, 1500, and 2000) and dust ratio values (density number N) of (2, 4, 6 and 8). A computer program in MATLAB has been built to carry out the numerical solution by writing the governing equation in finite difference method. The local Nusselt number, the average Nusselt number, the contours of temperature field and velocity field were presented to show the flow and heat transfer characteristics. The results show that when clean air flow, the wall temperature gradually increases along the cylinder length in the direction of flow and decrease as Reynolds number increase while it increases with input power. For dusty air flow results show that the wall temperature gradually increases along the axial direction and increase with Reynolds number and with input power, and the maximum reduction in heat transfer will be 30 % for N=8 at Re=2000. Comparison was made between the present experimental and numerical results and it gives good agreement. The experimental and numerical Nusselt number follows the same behavior with a mean deviation of 12%.

Key words: laminar, dusty air, forced convection, two dimensional, vertical annulus enclosure, glass beads.

الحمل القسري الطباقي لهواء مترب خلال وسط مسامي في محتوى حلقي عمودي

الاستاذ المساعد د. منال هادي الحافظ
كلية الهندسة - جامعة بغداد

سلمان حميد عبيد
كلية الهندسة - جامعة بغداد

الخلاصة

أجريت في هذا البحث دراسة عملية ونظرية لإنتقال الطاقة الحرارية بالحمل القسري بواسطة الهواء النقي أو المترب في فجوة حلقية ثنائية الأبعاد مملوؤة بوسط مسامي (كرات زجاجية) بين أسطوانتين عموديتين متحدتي المركز. القطرالخارجي للأسطوانة الخارجية (82mm) والقطر الخارجي للأسطوانة الداخلية (27 mm). تحت شروط حالة الإستقرار تم حفظ سطح الأسطوانة الداخلية بدرجة حرارية ثابتة وعالية بتسليط فيض حراري منتظم وتم حفظ سطح الأسطوانة الخارجية بدرجة حرارة الجو.شملت الدراسة قيم القدرة المدخلة (6.3, 4.884, 4.04 and 3.26 W) وعدد رينولد Re (300, 700, 1000, 1500, and 2000) وقيم نسب التراب N(2, 4, 6 and 8). تم بناء برنامج بلغة mat lab لتنفيذ الحل العددي باستخدام طريقة الفروق العددية. وتم

تمثيل عدد نسلت الموقعي وعدد نسلت المتوسط ومخططات المجال الحراري ومجال السرعة لتوضيح خواص الجريان وانتقال الطاقة الحرارية. أظهرت النتائج في حالة جريان الهواء النقي أن درجة الحرارة تزداد تدريجيا على طول الأسطوانة باتجاه الجريان وتقل بزيادة عدد رينولد بينما تزداد بزيادة القدرة المدخلة. نتائج جريان الهواء المترب بينت أن درجة الحرارة تزداد تدريجيا في الإتجاه المحوري وتزداد بزيادة عدد رينولد و القدرة المدخلة وأن أقصى انخفاض بانتقال الطاقة الحرارية يساوي % 30 لقيمة N=8وRe=2000. قورنت النتائج العملية والنظربة للبحث الحالي وأظهرت توافق جيد. نتائج عدد نسلت العملية والنظرية أظهرت السلوك ذاته بنسبة إنحراف 12%.

كلمات رئيسية : الطباقي, حمل قسري, هواء مترب, ثنائي الابعاد, محتوى حلقي عمودي, كرات زجاجية.

INTRONDUCTION

Fluid flow in a porous medium is a common phenomenon in nature, and in many fields of science and engineering. Important every day flow phenomena include transport of water in living plants and trees, and fertilizers or wastes in soil. Moreover, there is a wide variety of technical processes that involve fluid dynamics in various branches of process industry. The importance of improving our understanding of such processes arises from the high amount of energy consumed by them. In oil recovery, for example, a typical problem is the amount of unrecovered oil left in oil reservoirs by traditional recovery techniques ,**Aaltosalmi, 2005**. Flow through Convective heat transfer in porous medium has been intensively studied over the past two decades. This is because of its wide applications in geothermal energy engineering, ground-water pollution transport, nuclear waste disposal, chemical reactors engineering, insulation of buildings and pipes, storage of grain coal, **Kaurangini and Basant, 2009**.A lot of experimental and numerical study had been carried out in pure air and dusty air to investigate the heat transfer by forced convection by , **Cheng et al, 1988.** Analyzed the problem of a thermally developing forced convective flow in a packed channel heated asymmetrically. The flow in the packed channel was assumed to be hydrodynamically fully developed and was governed by the Brinkman-Darcy-Ergun equation with variable porosity taken into consideration. A closed - form solution based on the method of matched asymptotic expansions was obtained for the axial velocity distribution, and the wall effect on pressure drop was illustrated.

Al Zahrani and SuhilKiwan, 2008. investigated numerically the steady-state, laminar, axisymmetric, mixed convection heat transfer in the annulus between two concentric vertical cylinders using porous inserts. The inner cylinder was subjected to constant heat flux and the outer cylinder was insulated. A finite volume code was used to numerically solve the sets of governing equations. The Darcy–Brinkman–Forschheimer's model along with Boussinesq's approximation was used to solve the flow in the porous region. The Navier–Stokes equation was used to describe the flow in the clear flow region. The dependence of the average Nusselt number on several flow and geometric parameters was investigated. These include: convective parameter, λ, Darcy number, Da, thermal conductivity ratio, *K*r, and porous-insert thickness to gap ratio *(H/D)*. It was found that, in general, the heat transfer enhances by the presence of porous layers of high thermal conductivity ratios. It was also found that there is a critical thermal conductivity ratio on which if the values of Kr are higher than the critical value the average Nusselt number starts to decrease. Also, it found that at low thermal conductivity ratio $(Kr \approx 1)$ and for all values of λ the porous material acts as thermal insulation.

Kumar et al., 2011. studied the effect of Dusty fluid on MHD free convection flow past a vertical porous plate with heat and mass transfer taking Viscous and Darcy resistance terms into account and the constant permeability of the medium numerically and neglecting induced magnetic field in

comparison to applied magnetic field. The velocity, temperature, concentration and skin friction distributions are derived. It is observed that velocity of dusty fluid and dust particles increases with the increase in Gr (Grashof number), K (Permeability parameter), B (Dusty fluid parameter) and B1 (Dust particles parameter), but it decreases with the increase in M (Magnetic parameter).
In the present work an experimental and numerical investigation had been done to study the 2–dimensional laminar convection heat transfer in an annulus of two concentric vertical cylinders with clean or dusty air as working fluid. The annulus contains porous media (glass beads) and the inner cylinder heated to a constant wall temperature using constant heat flux. The outer cylinder kept at atmospheric temperature. In the numerical method the finite difference approximation is applied and a MATLAB program is built to solve these equations.

EXPERIMENTAL STUDY

The test section in the present work is indicated diagrammatically in **Fig.1.** A centrifugal blower (AUGUSTO CATTANI) of (2.5 cm) diameter was used to supply the air to the system. The dust concentrations were determined during tests by using electronic balance with an accuracy of 0.001 g**.** Dust concentration was calculated by measuring the difference in glass wool weight before and after test.
The dust was stored in a storage tank with a capacity accommodate a large amount of dust. The storage tank has three holes, One of these holes is used for air to inter the tank and then to balance the pressure between the test pipe and the dust storage tank which is called equilibrium pipe, the second hole used to feed the test system with fine dust, while the last one was closed tightly and used to refill the storage tank with dust. The storage tank is connected with a dust control valve to control the concentration of dust before entering the test system**.** The glass wool filter is a cylindrical vessel shaped of 2 cm thick and 12 cm inside diameter and 15 cm height. Glass wool filter was used to retention dust and to determine the concentration of dust. A flow meter was used in the range of (0 – 10 m^3/hr.) and linked with a plastic tube with a diameter of (1.9812cm)**.** Dusty air valve opened after measuring the dust concentration and the dusty air allowed passing to test section.
The test section consists of a Aluminum outer cylinders of (82 mm) outside diameters, (4 mm) thick and (260mm) long to which Aluminum inner cylinders of (27mm) outside diameter, (260 mm) long and (5 mm) thick; yield into radius ratios of 0.365 mm Aluminum was chosen because of its high thermal conductivity, available, cheap and for its easy machinability. The holder and the test rig are connected together and balanced to be vertical so that the inclination angle indicates to read zero. The inner cylinder was heated by passing an alternating current through a (0.25 mm) in diameter, (5m) long, 97 – ohm Nichrome wire coiled as spiral inside glass tube where glass tube was of (8mm) in diameter and (250 mm) long**.** The heater (i.e. the glass tube and the Nichrome wire) was mounted concentrically by two Teflon pieces. Teflon piece drilled to pass the working fluid and thermocouples wires, The inner cylinder was heated by passing an alternating current to a heater inside the inner cylinder and the outer cylinder was subjected to the surrounding temperature. The inner cylinder surface temperatures were measured at six locations using thermocouples type (K). The investigation covered values of input power of (6.3, 4.884, 4.04 and 3.26 W), Reynolds number values of (300, 700, 1000, 1500, and 2000) and dust ratio values (density number N) of (2 to 8).

MATHEMATICAL MODEL

The geometry and coordinate system of the problem considered are shown in **Fig. 2**. Convective heat transfer through a saturated porous media with dusty air flow is considered. The research is based on a series of concepts; such concepts include porosity, permeability of the porous medium, speed of dusty air through porous media, and the quantity of dust particles (called density number) in the fluid flowing through the medium. In order to model the incompressible flow in the porous medium of the steady-state equations. The governing equations are given as follow:

Mass conservation

The properties of both the fluid and saturated solid matrix are taken as constant, except the fluid density which defined the buoyancy in the momentum equation. Then the mass conservation can be written as **Shyamanta, 1998**.

$$\frac{1}{r}\frac{\partial}{\partial r}(r\,u)+\frac{\partial v}{\partial z}=0 \tag{1}$$

Momentum Equation

The equations of motion of a steady viscous incompressible fluid with uniform distribution of dust particles in a porous medium are given by, **Shyamanta, 1998 and AL-Sumaily et al., 2011.**

In R direction

$$\frac{u}{\in}\frac{\partial u}{\partial r}+\frac{v}{\in}\frac{\partial u}{\partial z}=-\frac{1}{\rho}\frac{\partial P}{\partial r}+\frac{\upsilon_{eff}}{\in}\left(\frac{\partial}{\partial r}\left[\frac{1}{r}\frac{\partial}{\partial r}(ru)\right]+\frac{\partial^2 u}{\partial z^2}\right)+\frac{k}{\rho}N\times u-\frac{\upsilon}{K}u \tag{2}$$

In z direction

$$\frac{u}{\in}\frac{\partial v}{\partial r}+\frac{v}{\in}\frac{\partial v}{\partial z}=-\frac{1}{\rho}\frac{\partial P}{\partial z}+\frac{\upsilon_{eff}}{\in}\left(\frac{1}{r}\frac{\partial}{\partial r}\left[r\frac{\partial v}{\partial r}\right]+\frac{\partial^2 v}{\partial z^2}\right)+\frac{k}{\rho}N\times v-\frac{\upsilon}{K}v \tag{3}$$

Energy Equation:

The most important law applied here is the first law of thermodynamic, and according to the assumptions the energy equation is , **AL-Sumaily et al., 2011.** :

$$\frac{\rho\, c_p}{\in}\left(u\frac{\partial T}{\partial r}+v\frac{\partial T}{\partial z}\right)=k_{eff}\left[\frac{1}{r}\frac{\partial}{\partial r}\left(r\frac{\partial T}{\partial r}\right)+\frac{\partial}{\partial z}\left(\frac{\partial T}{\partial z}\right)\right] \tag{4}$$

Where

C_p is specific heat of fluid at constant Pressure $(\frac{kJ}{kg.K})$.

Dimensionless Governing Equations

The advantage of non dimentionalization is that the minimum number of characteristic parameters results. Also the problem variables may be at the same time normalized. All spatial dimensions are nondimensionalized with respect to the gap D as follow ,**Shyamanta, 1998:**

$$V=\frac{v}{v_\infty}\qquad R=\frac{r}{Dh}\ ,\quad Z=\frac{z}{Dh}\qquad P=\frac{p}{\rho v_\infty{}^2}\qquad \theta=\frac{(T-T_\infty)}{(T1-T_\infty)}\ Re=\frac{v_\infty Dh}{\upsilon}\ U=\frac{u}{v_\infty}$$

$$N^*=\frac{C}{R_t},\qquad C=\frac{m\quad N}{\rho}\qquad R_t=\frac{m\ \ u_\infty}{k\ \ Dh}\ \gamma=\frac{\upsilon_{eff}}{\upsilon}\ ,Da=\frac{K}{Dh^2},R_K=\frac{k_{eff}}{k_f}$$

Where:

C = dust particle concentration.

R_t= relaxation time parameter of dust particle, **Shyamanta, 1998**.

Taking curl of momentum equations to eliminate pressure terms, the momentum and the energy equation will be:

$$\frac{1}{\in}\frac{\partial(U\omega)}{\partial R}+\frac{1}{\in}\frac{\partial(V\omega)}{\partial Z}=(N^*\in-\frac{\in}{\mathrm{Re}\,Da})\omega+\frac{\gamma}{\mathrm{Re}}\left(\frac{\partial}{\partial R}\left(\frac{1}{R}\frac{\partial(R\omega)}{\partial R}\right)+\frac{\partial^2\omega}{\partial\ Z^2}\right)\qquad(5)$$

$$\frac{1}{R\in}\left[\frac{\partial\Psi}{\partial Z}\frac{\partial\theta}{\partial R}-\frac{\partial\Psi}{\partial R}\frac{\partial\theta}{\partial Z}\right]=\frac{R_K}{\mathrm{Re}\ \mathrm{Pr}}\left[\frac{1}{R}\frac{\partial}{\partial R}\left(R\frac{\partial\theta}{\partial R}\right)+\frac{\partial^2\theta}{\partial Z^2}\right]\qquad(6)$$

$$V=-\frac{1}{R}\frac{\partial\psi}{\partial R}\qquad(7)$$

$$U=\frac{1}{R}\frac{\partial\psi}{\partial Z}\qquad(8)$$

$$-\omega=\frac{1}{R}\left(\frac{\partial^2\psi}{\partial R^2}-\frac{1}{R}\frac{\partial\psi}{\partial R}+\frac{\partial^2\psi}{\partial\ Z^2}\right)=\nabla^2\psi\qquad(9)$$

Dimensionless Hydraulic Boundary Conditions for stream lines

At R=$\frac{r_{in}}{Dh}$ and R=$\frac{r_{out}}{Dh}$

$$\psi(i,k)=\frac{4}{3}\psi(i,k+1)-\frac{1}{3}\psi(i,k+2)$$

At $Z=0,\ \ L$

$$\psi(i,k)=\frac{4}{3}\psi(i+1,k)-\frac{1}{3}\psi(i+2,k)+\frac{2}{3}R(k)\Delta R$$

Dimensionless Thermal Boundary Conditions

At $R=\frac{r_{in}}{Dh}$ $\theta_{(i,k)}=1$

At $R=\frac{r_{out}}{Dh}$ $\theta(i,k)=\theta_2$

At Z=0 $\theta(i,k)=0$

At Z=L $\theta(i,k)=\theta_{av}$

Calculation of Average Nusselt Number

The average Nusselt number on the walls cylinder can be calculated from the equation below:

$$N\bar{u}=-\frac{1}{l}\int_0^l Nu\ dZ \qquad (10)$$

Computational Technique

Eqs.(5, 6 and 9) were transformed into the finite difference equations, where the upwind differential method in the left hand side of the energy Eq. (6) and the centered – space differential method for the other terms were used, and solved by using (SOR) method ,**Wang and Zhang 1990**. A computer program was built using MATLAB to meet the requirements of the problem. The value of the stream line will be calculated at each node, in which the value of stream line is unknown, the other node will appear in the right hand side of each equation. As an initial value of iteration, zero is chosen for the stream line field, while a conduction solution is adopted for temperature field. The index (n) was used to represent the nth approximation of temperature denoted by Θ^n and substituted into the approximated equations, which were solved to obtain the nth –approximation of vorticity ω then substituted Eq.(5) to obtain stream line Ψ, then Ψ was substituted into Eq. (6) to obtain Θ^{n+1}. A similar procedure is repeated until the prescribed convergence criterion given by inequality:

$$Max\left|\frac{\theta^{n+1}-\theta^{n}}{\theta^{n}}\right| \leq 10^{-8}$$

The number of grid points used was 41 grid points in the R– direction and 301 in the Z – direction which seems reasonable and will be used in the present study. **Fig.3** illustrates the numerical grid in two planes.

Calculation of Local Nusselt Number

The local Nusselt number (Nu_l) on the walls can be found from the equation below:

$$Nu_l = \frac{h \times w}{k} \qquad (11)$$

The value of (h) can be found by making heat balance in the wall ,**Singh, 2003** as follow

$$q_{cond.} = q_{conv.} \qquad (12)$$

$$h(T_1 - T_\infty) = -k\left(\frac{\partial T}{\partial r}\right)_{r=0} \qquad (12)$$

Then:
From Nusselt number definition and dimensionless magnitudes:

$$Nu = -\left(\frac{\partial \theta}{\partial R}\right) \qquad (13)$$

The local Nusselt number *Nu* on the inner walls was expanded in form of finite difference approximation using backward difference scheme, **Anderson et al., 1984.**

$$Nu = \frac{-3\theta_{i,k} + 4\theta_{i-1,k} - \theta_{i-2,k}}{2\,\Delta R} \qquad (14)$$

RESULTS AND DISCUSSION

Fig.4 shows the temperature distribution for the case of clean air (N=0) through porous media for different values of Re. This figure illustrates that the temperature decreases with the Increase of (Re) and this is because increasing (Re) yields faster flow through the porous media over the heated wall .When the case of dusty air flow (for different values of dust ratio (N)) through porous media in the annulus and it is clear increase the temperature and increasing the dust ratio (N) leads to an additional increase in temperature. The porous medium affecting flow and heat transfer characteristics and it represents an additional resistance to the flow when compared with clear fluid flows.

Fig.5 shows the Z – component of the streamlines, in the (R-Z) plane for the cases of clean air and dusty air respectively. it is clear that intensity of streamlines increases in upper and lower surfaces of the annulus due to increase in Reynolds number (Re) and the intensity of streamlines decrease when the concentration of dusty air increase. Contours of velocity field in the (R-Z) plane are illustrated in **Fig.6** along the length of the annulus in (Z) direction. Flow illustrates symmetry in both sides of annulus and it is clear that its value in the bottom of the annulus is positive and in the upper is negative.

Fig.7 illustrates the case of dusty air flow through porous media in the annulus and it is clear that increasing the Reynolds number for constant dust ratio leads to increase the temperature and increasing the dust ratio (N) leads to an additional increase in temperature.

Fig.8, shows that the average Nusselt number for clean air increase with the increase of Reynolds number Re at constant heat flux. The average Nusselt number for dusty air decrease with Re and increasing the dust ratio cause an addition decrease in Nu as discussed previously.

The local Nusselt number depends on the temperature distribution along the cylinder length. **Fig.9** show that the local Nusselt number decreases gradually with the axial distance of the heated wall to about halve the length then became constant. The local Nu begin with high value at the inlet of entry length region due to the high difference between the air and the heated wall temperature, then progressively the difference between air and heated wall decreases. In experimental results **Fig.10** illustrates for the dusty air flow in annulus that the Nusselt number decreases with the increase of Reynolds number at constant heat flux and dust ratio. as well as the Nusselt number decreases with the increase of dust ratio at the same value of Reynolds number for constant heat flux.and it is clear that the Nusselt number increase with the increase of Reynolds number at constant dust number for different heat flux values and it is clear that as the heat flux increase the Nusselt number increase.

In **Fig.11** a comparison between the experimental and numerical results of the present work had been done for the variation of the Nusselt number with Reynolds number for clean air and dusty air with different dust ratios. The results of comparison show that the present experimental results follow the same behavior as the numerical results, with a deviation of (12%).

CONCLUSIONS

1. When clean air flow the wall temperature in the radial direction decreases as Reynolds number increases and the heat transfer decreases. For dusty air the wall temperature in the radial direction increase as Reynolds number increases and an addition increase was observed when dust number N increase.
2. The maximum percent reduction in heat transfer is 14.1 for N=8 at Re=2000.
3. The local Nusselt number decrease gradually along the length of the cylinder.
4. The average Nusselt number increases as the Reynolds number increases for clean air flow at constant heat flux.
5. The average Nusselt number decrease as the Reynolds number increases for dusty air flow at constant heat flux.
6. Comparison shows good agreement between the present and previous works.

REFERENCES

- Aaltosalmi U ,2005 *Fluid Flow in Porous Media with the Lattice – Boltzmann Method* PhD. Thesis, University of Jyväskylä on July 29, .

- Al-Sumaily Gazy F , John Sheridan, Mark C. Thompson,2012. *Analysis of forced convection heat transfer from a circular cylinder embedded in a porous medium* International Journal of Thermal Sciences 51 - 121-131.

- Al Zahrani and SuhilKiwan ,2008. *Mixed Convection Heat Transfer in the Annulus Between Two Concentric Vertical Cylinders Using Porous Layers* , J. of Transp Porous Med 76:391–405.

- Anderson A. A., Tannehill,C. J. and Pletcher H. R.1984, *Computational Fluid Mechanics and Heat Transfer*, McGraw – Hill book company/ Hemisphere Publisher.

- Cheng P., Hsu C.T. and Chowdhury A.,1988, *Forced Convection in the Entrance Region of Packed Channel with a Symmetric Heating* , Transactions of the ASME, Vol. 110, pp. 946 - 954.

- Kaurangini M.L. andBasant . K, 2009, *Mixed Convection Flow in A Vertical Annulus Filled with Porous Material Having Constant Porosity* , Techno Science Africana Journal, Volume 3 Number 1, June.

- Kumari M. and. Nathb G.,2008, *Unsteady Natural Convection from a Horizontal Annulus Filled with a Porous Medium*, Int. J. of Heat and Mass Transfer, Vol, 51, pp. 5001–5007. www.elsevier.com.

- Shyamanta, 1998, *MHD Flow and Heat Transfer of A Dusty Viscoelastic Stratified Fluid Down an Inclined Channel in Porous Medium Under Variable Viscosity*, Theoretical and applied mechanics ,vol.26,PP.1-14 .

- Singh N. P. and Ajay Kumar Singh, 2003, *MHD Free Convection and Mass Transfer Flow Past a Flat Plate*, the Arabian Journal for Science and Engineering, vol. 32, number 1A .

- Wang Bu – Xuan and Zhang Xing,1990 "*Natural Convection in Liquid Saturated Porous Media Between Concentric Inclined Cylinders*" Int. J. Heat and Mass Transfer Vol. 33. No 5, pp. 827-833.

NOMENCLATURE

Letter	Description	Units
C_p	Specific heat at constant pressure	kJ/kg °K
d_o	Outer diameter of the inner cylinder	M
dg	Diameter of glass bead	mm
Da	Darcy number $Da=K/Dh^2$	-
D_i	Inner diameter of the outer cylinder	m
D_h	Annulus diameter (D_i_ d_o)	m
h_i	The convection heat transfer coefficient on the inner cylinder (hot surface)	W/m^2K
$K_{eff.}$	Effective thermal conductivity of the porous media	W/m K
k_f	Thermal conductivity of the fluid	W/m K

k_s	Thermal conductivity of the solid	W/m K
K	Permeability	m^2
l	Cylinder length	m
L	Dimensionless cylinder length	-
N	Dust ratio	g/min
N^*	Dimensionless dust ratio	-
Nu_1	Local Nusselt number on the inner cylinder $Nu_1 = -\left(\frac{\partial \theta}{\partial R}\right)_1$	-
p	Pressure	N/m^2
P	Dimensionless pressure	-
Q	Input power	W
Q	Convective heat transfer rate	W
$Q_{cond.}$	Heat loss by conduction	W
r	Radial coordinate	m
r_{in}	Radius of the inner cylinder	m
r_{out}	Radius of the outer cylinder	m
R	Dimensionless radial coordinate	m
Re	Reynolds number	$Re = \frac{V\ Dh}{\upsilon f}$
Rr	Radius ratio $Rr=r_{in}/r_{out}$	-
Pr	Prandtl number($Pr=\nu/\alpha$)	—
T	Temperature	K
T_∞	Ambiant temperature	K
T_1	Temperature of the inner cylinder surface	K
T_2	Temperature of the outer cylinder surface	K
T_{ave}	Average temperature($(T_{1+} T_2)/2$)	K
u	Radial velocity component	m/s

v	Axial velocity component	m/s
v_∞	Velocity of air in Axial direction	m/s
U	Dimensionless velocity component in R -direction	-
V	Dimensionless velocity component in Z -direction	-
w	Gap width ($r_{out} - r_{in}$)	m
x, y, z	Cartesian coordinate system	m
Z	Dimensionless axial coordinate	-

Greek Letters

Letter	Description	Units
α	Thermal diffusivity	m^2/s
$\alpha_{eff.}$	Effective thermal conductivity of the porous media	m^2/s
β	Volumetric thermal expansion coefficient	1/K
ε	Porosity	-
θ	Dimensionless temperature	-
γ	Dimensionless kinematic viscosity	-
R_K	Dimensionless thermal conductivity	-
μ_f	Dynamic viscosity of fluid	$N.s/m^2$
ρ_f	density of fluid	kg/m^3
t	Time	s
υ_f	Kinematic viscosity of the fluid	m^2/s
ψ	Streamline	-
ω	Dimensionless vorticity	-
ΔR, ΔZ	Distance between the grid points	-

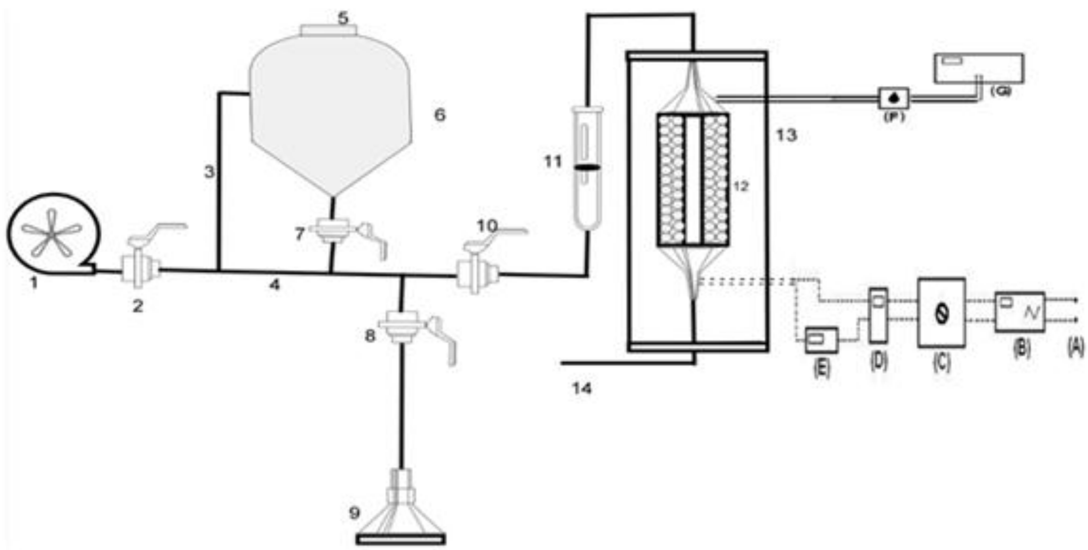

1-Blower 2- flow control valve 3- equilibrium pipe 4- main pipe 5- hole to refill dust
6- dust storage tank 7- dust control valve 8- retention dust valve 9- glass wool filter
10- dusty air valve 11- flow meter 12- vertical annulus With porous media
13- Outer cover 14- outlet pipe A- power supply B- stabilizer C- variac
D- Voltmeter E- Ammeter F- selector switch G- digital thermometer ,
-------- Heater Circuit , ———— Thermocouple Circuit

Figure 1. Schematic diagram of experimental apparatus.

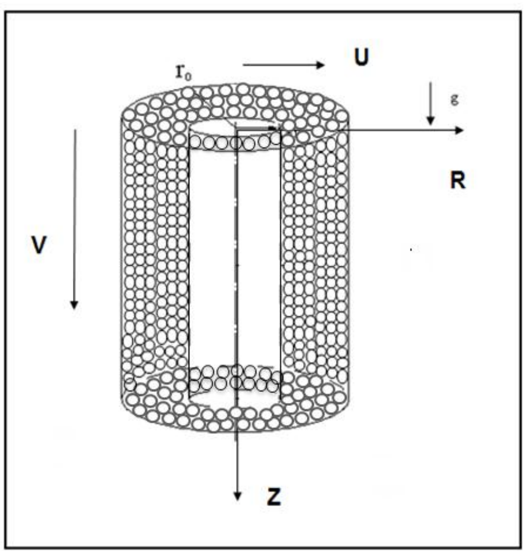

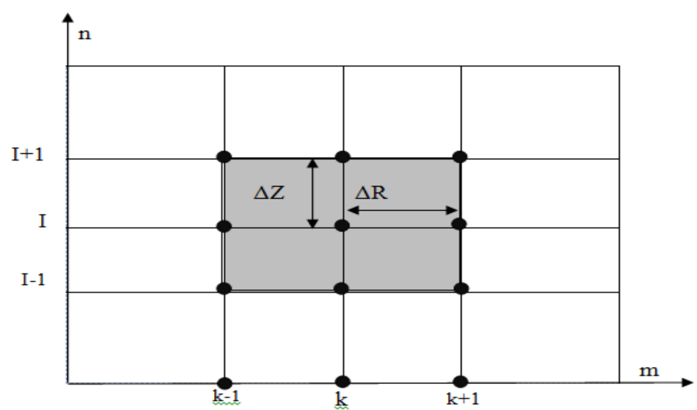

Figure 3 . A Plot of two dimensional discretized domains.

Figure 2 . Geometry and coordinates system.

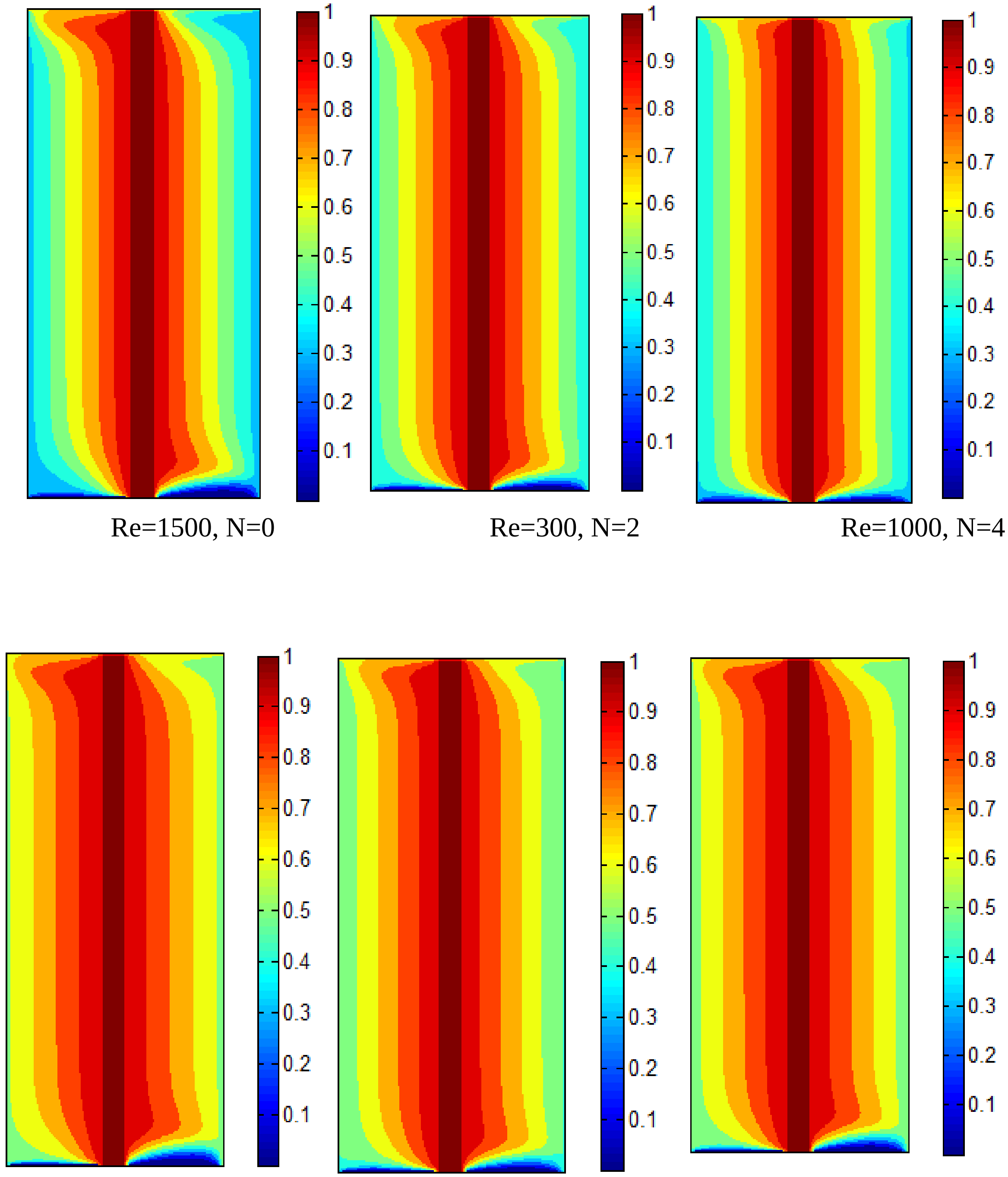

Re=1500, N=0 Re=300, N=2 Re=1000, N=4

Re=1000, N=6 Re=300, N=8 Re=200, N=8

Figure 4. Temperature distributions.

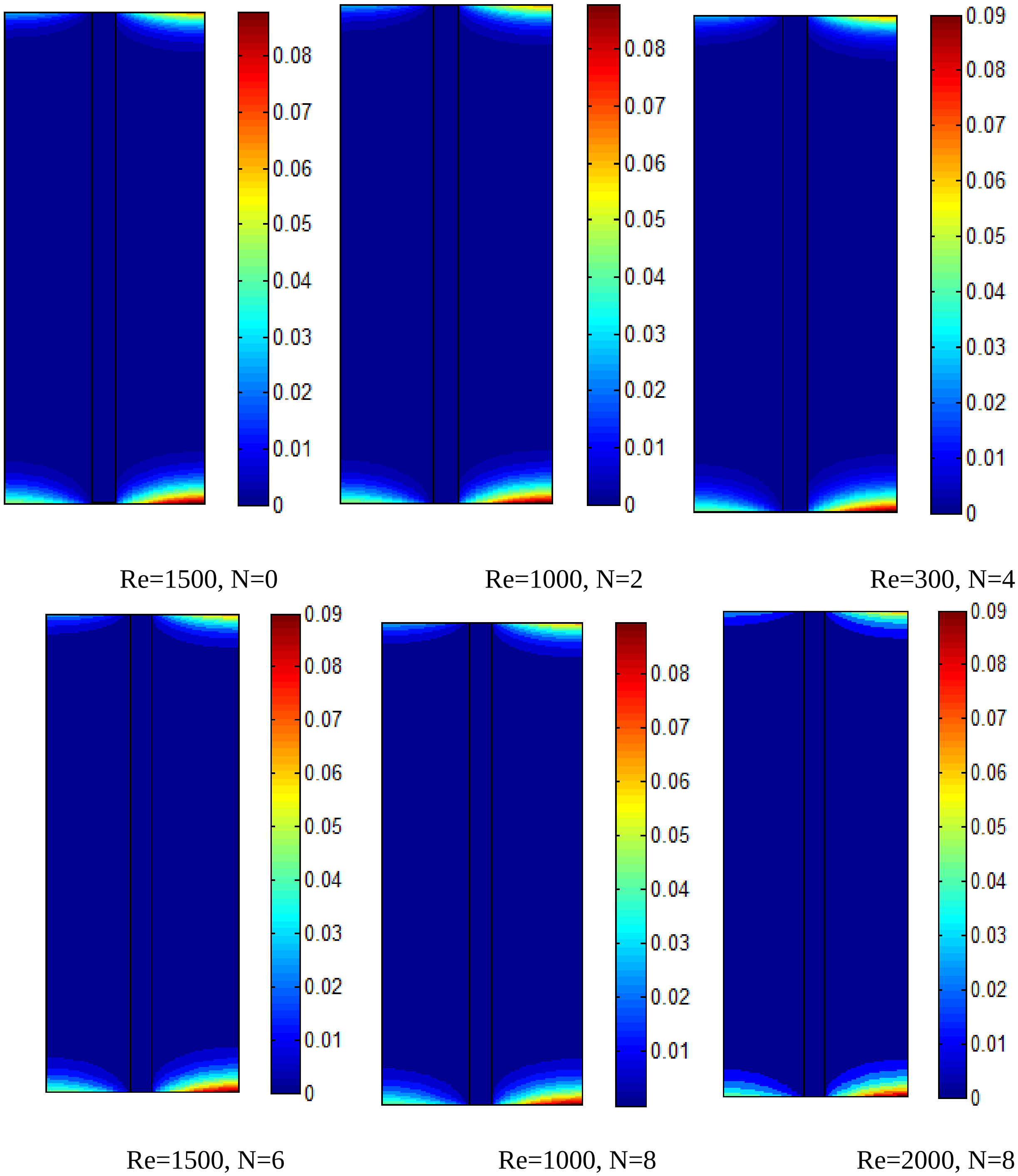

Figure 5. Contours of streamlines (*ψ)*.

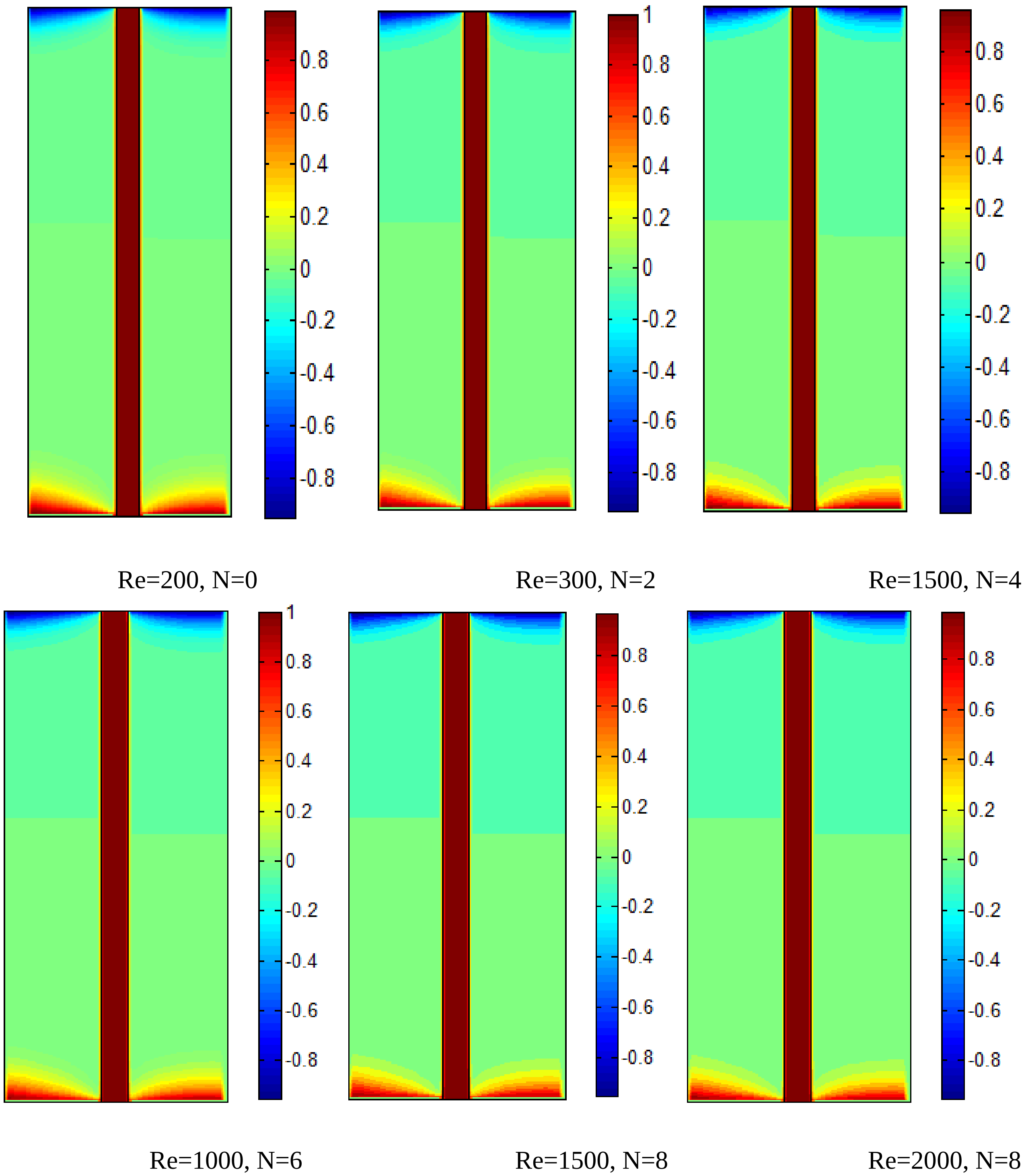

Figure 6 . Velocity field (V) in axial direction.

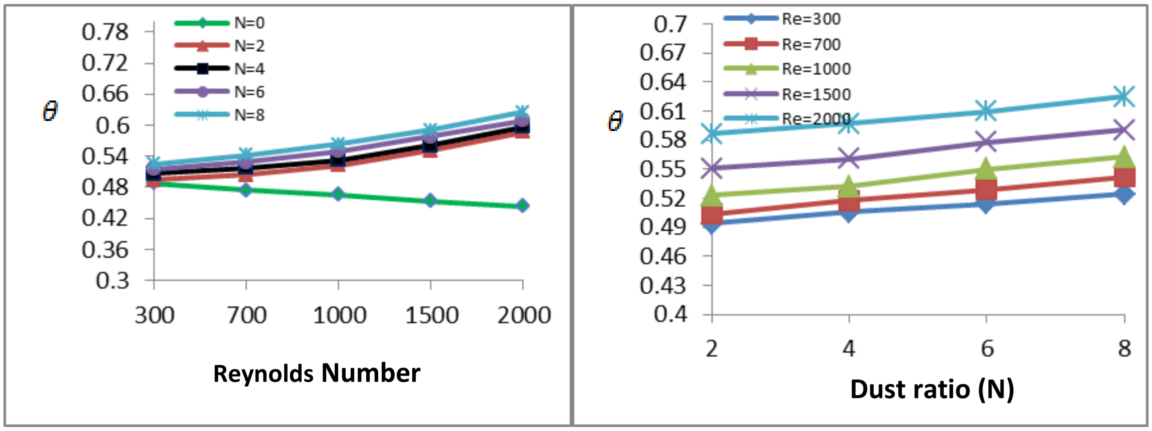

Figure 7. Variation of (θ) with (N) and with (Re).

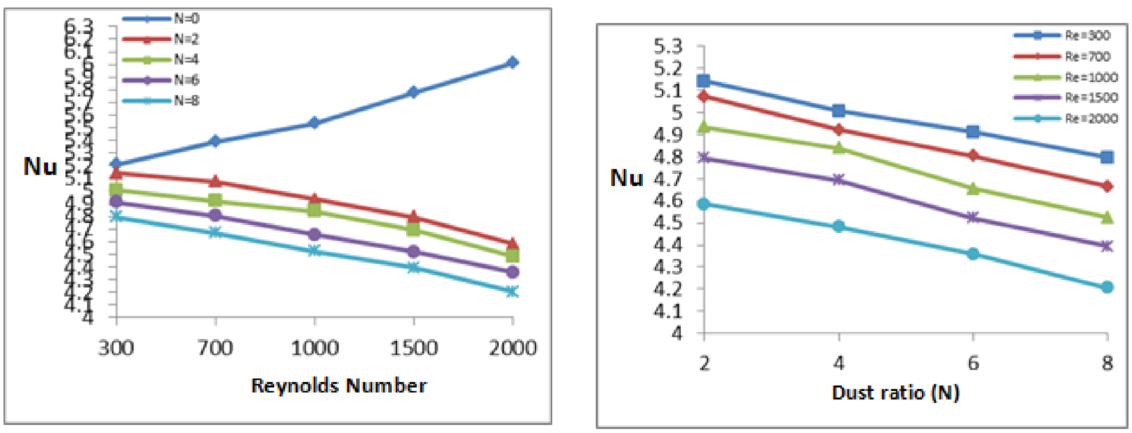

Figure 8. Variation of (Nu) with (N) and with (Re).

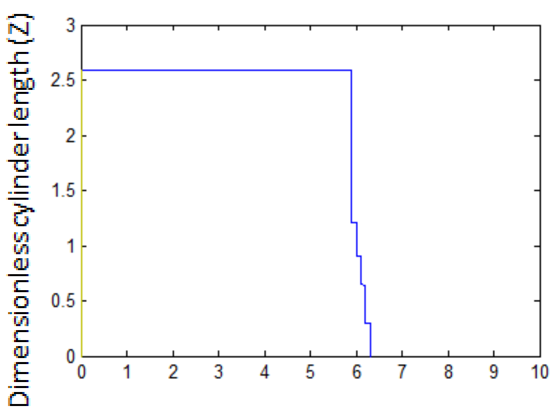

Local Nusselt number(N=0, Re=1000)

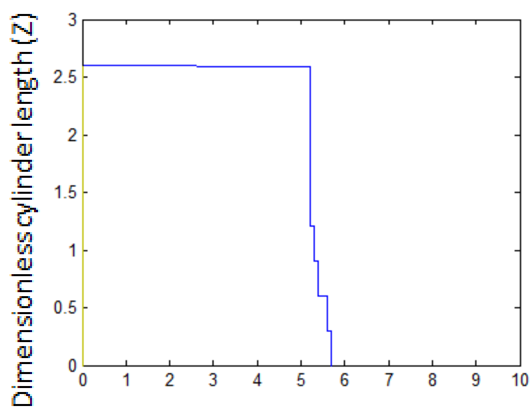

Local Nusselt number(N=0, Re=2000)

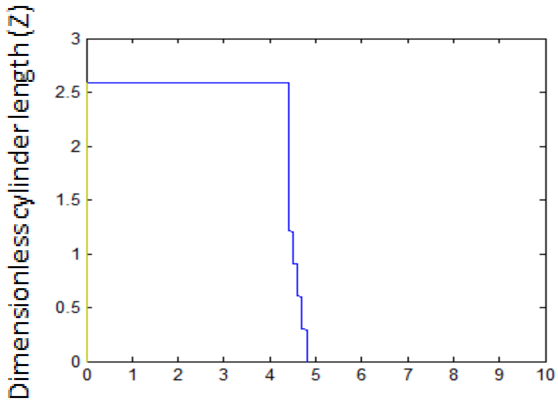

Local Nusselt number(N=4, Re=700)

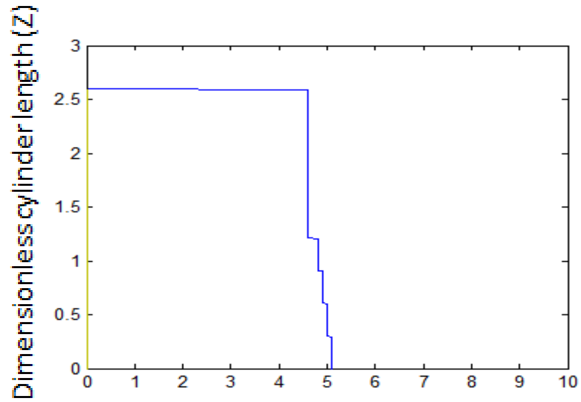

Local Nusselt number(N=8, Re=1000)

Figure 9. Variation of local Nusselt number in (Z – Direction) along the hot cylinder.

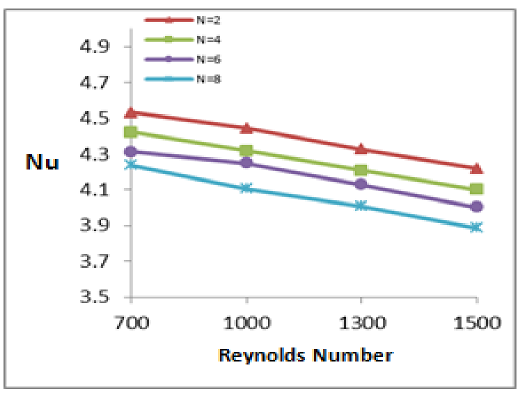

Q=6.3W

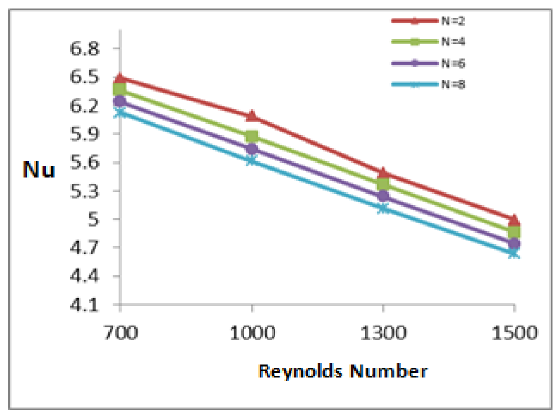

Q=4.884W

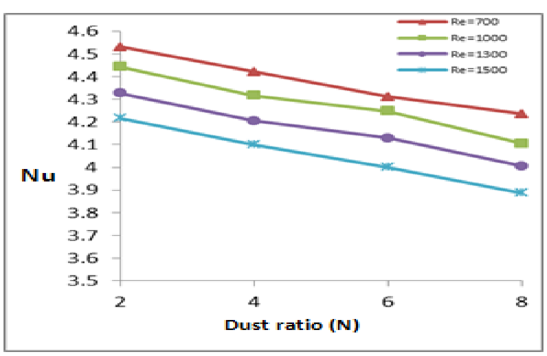

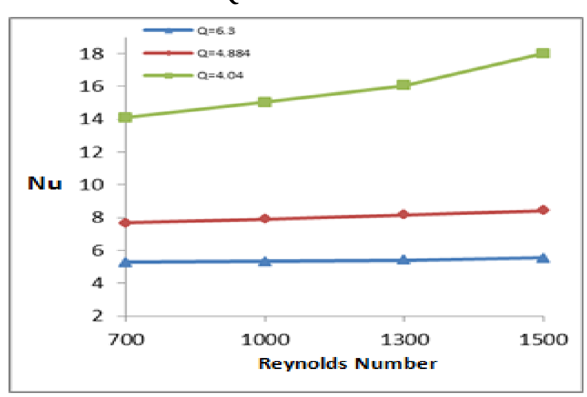

Q=6.3W clean air (N=0)

Figure 10. Experimental variation of average Nusselt number with Reynolds number and Dust ratio.

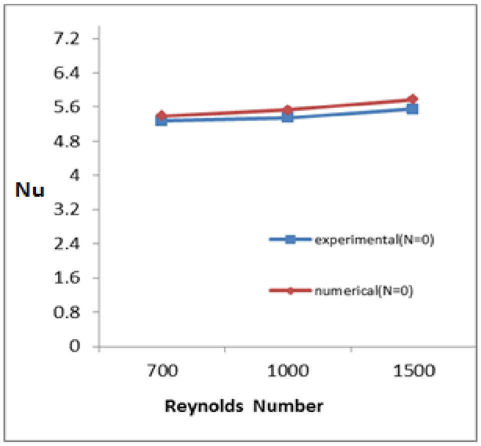

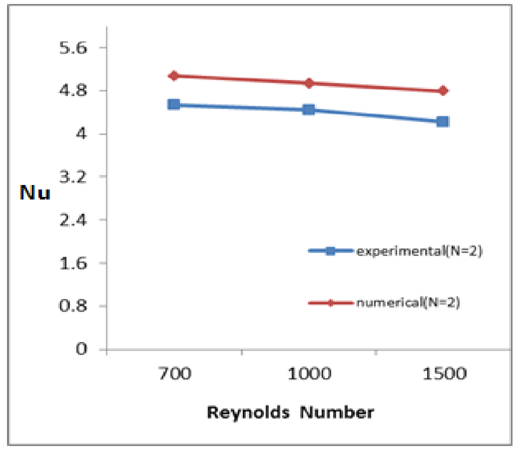

Figure 11. Comparison of Experimental and Numerical Results.